

Fullerene Evolution in Flame-Generated Soot

P. T. A. Reilly,* R. A. Gieray, W. B. Whitten, and J. M. Ramsey

Contribution from the Oak Ridge National Laboratory, 4500S MS-6142 P.O. Box 2008, Oak Ridge Tennessee 37831-6142

Received February 22, 2000

Abstract: Direct observation of the chemical evolution of flame-generated soot was demonstrated for the first time using real-time aerosol mass spectrometry. The data presented unambiguously show the transformation of particle phase polycyclic aromatic hydrocarbons (PAHs) into carbonaceous soot containing fullerenes. The mechanism of fullerene formation in the particle phase that is revealed is not consistent with conventional gas-phase formation mechanisms. This mechanism suggests the possibility of a controlled condensed phase synthesis of fullerenes.

Since Kroto et al.¹ first suggested the truncated icosahedral structure of C₆₀, flames have been examined for fullerene growth. Experimental investigations into the formation of fullerenes in flames have primarily focused on species found in the gas phase^{2–4} or extracts from bulk collected soot.^{5,6} Until now, no real-time measurements have directly examined the soot particle phase for fullerene growth. In this article, it will be demonstrated that individual soot particles can be sampled without significant quantities of the gas-phase combustion species condensing on them.⁷ That is, gas-phase condensation on the particles and particle agglomeration that result from the sampling process do not significantly affect the individual particle mass spectra. Moreover, it will also be shown that this technique can reveal the chemical evolution of the fullerenes in the particle phase because it can track the change in composition over the entire ensemble of measured particles.

The size and composition of each of the individual soot particles in the flame is the result of its environmental history. In the experiments presented here, the particles sampled from the flame have a sweeping range of environmental histories because they were sampled across the entire lateral cross section of the flame. Because the particle composition is the result of its previous environment, sorting the particles according to their composition permits better understanding of soot particle evolution. The following discussion presents the methodology used to sort the collected individual soot particle spectra and determine the evolutionary path of fullerenes in the particle phase of an atmospheric acetylene diffusion flame.

* To whom correspondence should be addressed.

(1) Kroto, H. W.; Heath, J. R.; O'Brien, S. C.; Curl, R. F.; Smalley, R. E. *Nature* **1985**, *318*, 162.

(2) Baum, T.; Löffler, S.; Löffler, P.; Weilmünster, P.; Homann, K.-H. *Ber. Bunsen-Ges. Phys. Chem.* **1992**, *96*, 841.

(3) Ahrens, J.; et al. *Int. J. Mass Spectrom. Ion Processes* **1994**, *138*, 133.

(4) Weilmünster, P.; Keller, A.; Homann, K.-H. *Combust. Flame* **1999**, *116*, 62.

(5) Howard, J. B.; McKinnon, J. T.; Makarovskiy, Y.; Lafleur, A. L.; Johnson, M. E. *Nature* **1991**, *352*, 139.

(6) McKinnon, J. T.; Bell, W. L.; Barkley, R. M. *Combust. Flame* **1992**, *88*, 102.

(7) Condensation and agglomeration are not substantial in our sampling process as evidenced by the observed compositional evolution shown later in the article.

Experimental Section

The experimental apparatus used for real-time particle measurement has been described in detail elsewhere.^{8–12} The burner used in these experiments consisted of four 1.1-mm i.d., 1.5-mm o.d., 65-mm long brass tubes clustered together in a square pattern soldered into a brass plug yielding a torch-like flame. The flow rate of the pure acetylene through the tubes was approximately 2.4 cm³/s. No oxygen or air was premixed with the acetylene. The resulting smoking atmospheric diffusion flame was approximately 11 cm in height and 8 mm in diameter. A 4-in. diameter exhaust snorkel was located above the flame to collect the smoke. Particles were sampled at one height in the flame, approximately 30 mm above the burner, through a 3.2-mm o.d., 1.4-mm i.d., and 6.0-cm long stainless steel tube connected to a 250-mL chamber that was used as a holding chamber to permit dilution of the aerosol and sedimentation of large soot particles. No special attempt was made to cool the sampling tube. A second inlet to the dilution chamber allowed the particle stream to be diluted with room air to reduce clogging of the particle inlet, gas-phase condensation, and particle agglomeration. The output of the dilution chamber was connected to the particle inlet of the apparatus using 3.2-mm i.d. tubing. The residence time in the dilution chamber and tubing is 10 s. The time spent in a vacuum traveling from the inlet opening to the center of the ion trap where the particles are ablated and ionized is less than 1 ms so that vacuum-induced evaporation of volatile species is not significant. Because of the size of the sampling tube relative to the width of the flame and the lack of a coannular sheath of air shielding the flame from room air currents, particles were sampled from a complete cross section of the flame and hence the sampled particles had widely varying histories. The flame particles were sampled in short pulses by briefly blocking then unblocking the second inlet on the dilution chamber. The apparatus inlet draws 42 cm³/s; consequently, major portions of the flame were drawn into the sampling tube with a minimum factor of 17.5 times the volume of air. This caused immediate quenching of the flame at the point where it was drawn into the sampling tube. (Proof of complete mixing and quenching of the flame upon sampling can be found in ref 12—see endnote 18 therein. This

(8) Gieray, R. A.; Reilly, P. T. A.; Yang, M.; Whitten, W. B.; Ramsey, J. M. *Anal. Chem.* **1998**, *70*, 117.

(9) Reilly, P. T. A.; Gieray, R. A.; Whitten, W. B.; Ramsey, J. M. *Environ. Sci. Technol.* **1998**, *32*, 2672.

(10) Gieray, R. A.; Reilly, P. T. A.; Yang, M.; Whitten, W. B.; Ramsey, J. M. *J. Microbiol. Methods* **1997**, *29*, 191.

(11) Reilly, P. T. A.; Gieray, R. A.; Yang, M.; Whitten, W. B.; Ramsey, J. M. *Anal. Chem.* **1997**, *69*, 36.

(12) Reilly, P. T. A.; Gieray, R. A.; Whitten, W. B.; Ramsey, J. M. *Combust. Flame* **2000**, *122*, 90.

proof was derived by showing that if the flame were a room temperature aerosol then the mixing would still be turbulently completed in the sampling tube and by further recognizing the large enhancement that results from thermophoretic mixing of two vastly different temperature streams.) Upon exiting the sampling tube, the particles were further diluted with room temperature air already in the chamber and air continuously being sucked through the chamber at 42 cm³/s. During the course of the experiments, the temperature of the dilution chamber did not significantly rise above room temperature so that no further oxidation of the particles occurred in the dilution chamber. The rapid quenching of the flame-induced pyrolysis and dilution permitted the flame borne particles to be sampled without significant condensation of the flame borne gaseous species. In other words, the amount of gaseous flame borne material condensed on the particles as a result of the sampling process is not significant in comparison to the amount of material ablated from the particle as will be demonstrated by analysis of the data. Further proof of the validity of our sampling method can be found in a companion study on soot formation¹² and was obtained by optical microscopy performed on soot particles sampled directly from the flame and immediately after the sampling tube by impaction. These results clearly show the presence of optically transparent globular micrometer-sized particles as well as mature soot aggregates before and after the sampling tube. They confirm the results of Sorensen and Feke,¹³ who studied the morphology of macroscopic soot produced from a similar acetylene diffusion flame. As yet unpublished results from laser microprobe mass spectrometry further confirm the validity of the sampling technique and conclusively demonstrate that the laser does not cause the evolution shown in this publication and ref 12.

Particles entered the main vacuum chamber of the apparatus through a differentially pumped inlet and were detected by light scattering at two separate points. Timing electronics recorded the time-of-flight between the two detection points and triggered a focused 308 nm excimer laser ((1–2) × 10⁸ W/cm²) to ablate and ionize the particle when it reached the center of the trap regardless of particle size or velocity. The ablation laser intensity used is enough to ablate substantial portions of the particle (i.e., not just the first few layers). The time-of-flight between the detection points directly correlates with particle size. Therefore, the particle size was recorded with each particle mass spectrum.

Results and Discussion

Particle size and mass spectra for three separate runs of one thousand soot particles each were collected. Our aerodynamic sizing measurements revealed a narrow distribution (200 nm at full width half-maximum) that peaks at 750 nm. Two thousand soot particles were analyzed to determine the evolution of the carbonization process as described by Dobbins et al.¹⁴ Of these, 1440 had sufficient relative total ion counts (RICs) to yield useful spectra. The rest were rejected and interpreted as misses by the ablation laser. While examining the individual mass spectra, it was noticed that the spectra predominantly composed of PAH mass lines yielded much lower RICs than the spectra predominantly composed of carbon cluster ions. (Note: Soot particles that predominantly yield PAH ions are referred to as PAH-containing soot and soot particles that predominantly yield carbon cluster ions are referred to as mature or carbonaceous soot.) It was soon realized that the composition of the soot particle or rather the amount of carbon cluster ions in the soot particle spectrum (i.e., the degree of soot particle carbonization as we define it) correlated with RIC. Therefore, the 1440 spectra were then sorted as a function of RIC into six bins containing 240 spectra. Each bin was then averaged and the results are shown in Figure 1a–f.

The averaged spectra in Figure 1 showed a definitive compositional evolution from PAH-containing to mature soot

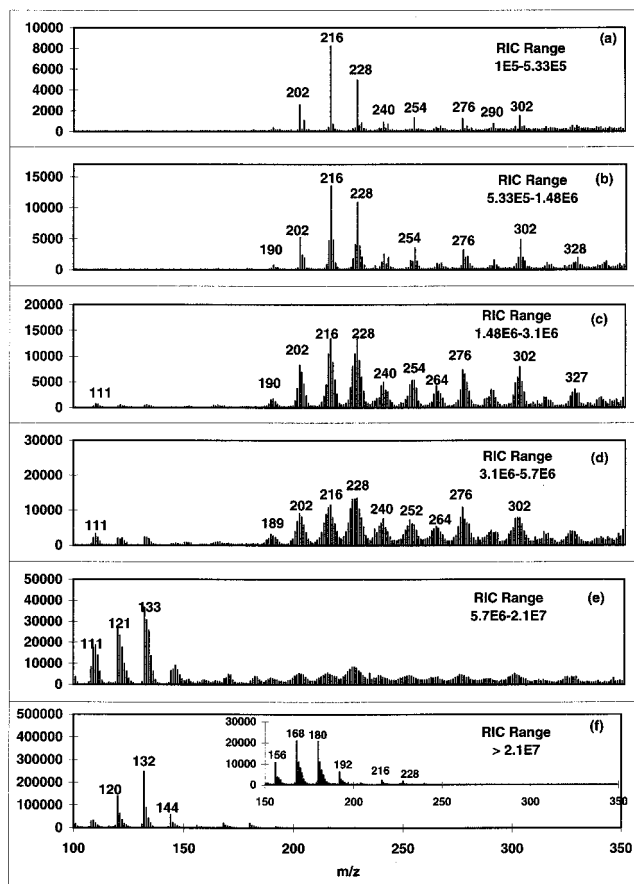


Figure 1. The individual particle mass spectra sorted and averaged as a function of RIC demonstrate the compositional evolution of the carbonization process (see text for details). The inset in panel f has the same as panel d.

particles¹⁵ that is the result of sampling different pyrolytic environmental paths in the flame because the entire lateral cross section of the flame was sampled. The evolution observed here correlates directly with the so-called carbonization process observed by Dobbins et al.¹⁴ The evolution shown in this figure also proves that sampling-induced condensation and aggregation do not significantly affect the particle mass spectra because, if it did, the observed heterogeneity in the spectra would be washed out. This point was demonstrated in a companion study on soot formation¹² where micrometer-sized globules and mature soot aggregates were shown to coexist in the flame by impact sampling and optical microscopy. Panel a shows apparently unpyrolyzed PAHs from particles that presumably traveled along the centerline of the diffusion flame where the oxygen concentration was minimal and the overall flame temperature was the lowest. The PAH-containing particles that presumably experienced hotter paths in the flame (i.e., further and further from the centerline of the diffusion flame) show signs of rapid exchange of hydrogen between the PAHs as witnessed by the dramatic increase in the intensities of the masses immediately surrounding the PAH peaks (see panels b, c, and d). Along with this process, the PAH molecules undergo a pyrolytic addition process that is evidenced by a growth in the intensity of the higher mass PAH ions (compare for example the change in the ratio of m/z 302 to 216 over the first three panels in Figure 1). The pyrolytic process reaches a point where rapid gain and loss of hydrogen permits rearrangement of the carbon skeleton of

(13) Sorensen, C. M.; Feke, G. D. *Aerosol Sci. Technol.* **1996**, *25*, 328.

(14) Dobbins, R. A.; Fletcher, R. A.; Chang, H.-C. *Combust. Flame* **1998**, *115*, 285.

(15) PAH and carbon cluster composition was verified by tandem mass spectrometry.

the PAH. At this point, the small carbon cluster ions begin to grow very rapidly while PAH ion intensity drops at the same rate over the last two panels revealing the direct conversion from PAH-containing to mature soot as defined by Dobbins et al.¹⁴ The mature soot particles have experienced the hottest paths in the flame, presumably the outermost portions of the flame where the O₂ concentration is the highest, while the PAH-containing soot presumably forms on the inside of the flame where the paths through the flame are cooler. In our companion study,¹² we suggested that PAH deposition in the flame occurs by a chemical bond forming process. This concept is supported by the distribution of the PAHs in the particles. The vapor pressures of the majority of PAHs that are found in the soot (<300 Da) are well above atmospheric pressure at the temperatures at which the PAH-containing particles are formed. Further examination of the PAH distribution in the apparently uncarbonized PAH-containing soot reveals hydrogenated PAHs¹⁶ at *m/z* 204, 254, and 302 and a dearth of intensity at *m/z* 252 and 300 contrary to what is normally seen for PAH-containing soot analysis by off-line techniques.^{14,17}

The possibility that the assignment of hydrogenated PAHs to the above masses may well be nonhydrogenated PAHs has been considered. For example, *m/z* 204 and 254 could be PAH dimers, phenylanthracene, and binaphthalene, respectively, while the *m/z* 302 peak could be any of the many PAHs isomers at that mass. However, our assignment of hydrogenated PAHs to these mass lines is based on many factors, not just possible isomer configurations. The first and perhaps most profound piece of evidence is the complete lack of benzopyrene type PAHs at *m/z* 252 and the unexpected presence of an abundance of the *m/z* 254 PAH in our "unpyrolyzed" PAH-containing real-time soot spectrum. When we look at unpyrolyzed PAH-containing soot droplets by laser microprobe mass spectrometry (LMMS) we see *m/z* 250 and 252 but no 254 from the same experiment. Our off-line LMMS results parallel those seen by Dobbins et al.¹⁴ in their study of precursor soot. This time-induced disappearance of *m/z* 254 with a corresponding appearance of the expected *m/z* 252 PAH cannot be explained by any suggestion other than hydrogenated PAHs. Furthermore, we have made MS/MS measurements on *m/z* 252 and 254 in our laboratory. The product ion spectrum from *m/z* 254 showed no *m/z* 127 ions; therefore, binaphthalene could not be a component of the parent ion. More importantly, the ability to rapidly exchange hydrogen between the PAHs in the PAH-containing soot, as clearly indicated by the spectra in Figure 1, necessitates the ability to store hydrogen. This hydrogen storage ability manifests itself by the presence of hydrogenated PAHs. Finally, when analyzing the mass spectra of hydrocarbons produced by pyrolysis or in the analysis of hydrocarbons in fuels or oils, it is important to consider the overall homologous series that are present in the ion distributions. The presence of dimer PAHs was specifically looked for in the high mass range and they were not observed (see Figure 2). For this reason, it is not expected that they would be found in the lower mass range shown in Figure 1a. From the above reasoning, we have concluded that hydrogenated PAHs exist in the "unpyrolyzed" PAH-containing droplets and more importantly that these PAHs show evidence of preferential hydrogenation.

The distribution of hydrogenated species shown in Figure 1a cannot be explained by gas-phase reactions because, in the gas phase, the probability of hydrogenation increases with increasing PAH size and should not be PAH discriminate.¹⁸ Therefore,

(16) Confirmed by tandem mass spectrometry.

(17) Tregrossi, A.; Ciajolo, A.; Barbella, R. *Combust. Flame* **1999**, *117*, 553–561

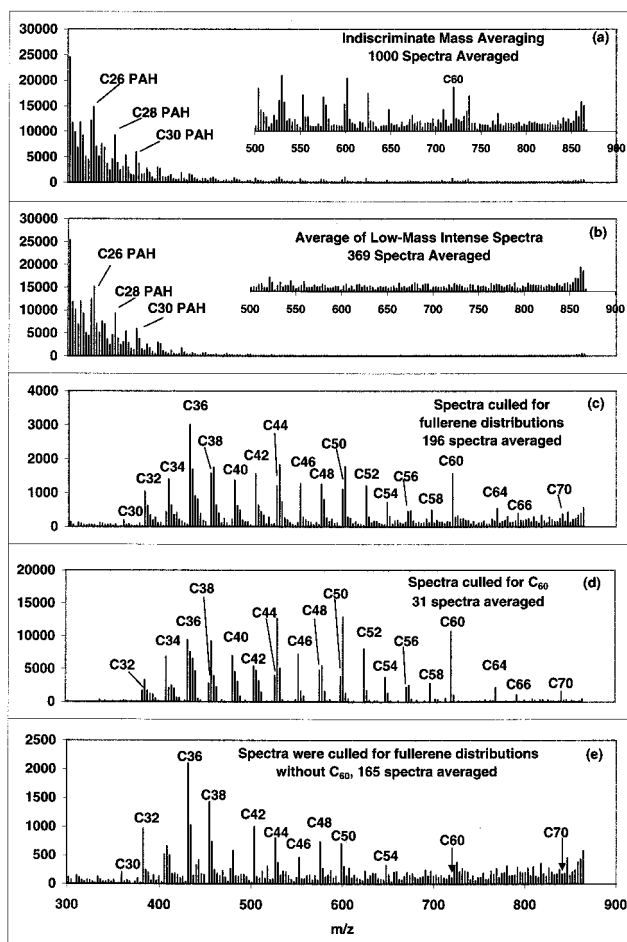


Figure 2. The averages of the individual particle mass spectra shown demonstrate the methodology used to observe fullerene evolution in the particle phase.

the observed PAH distribution is not the result of formation in the gas phase followed by physical condensation that would result from the sampling process (this latter process defines sampling-induced condensation). In addition, it is well-known that the *m/z* 252 PAH exists in easily observable quantities in the gas phase for essentially all flame systems. If the mass spectra were significantly affected by sampling-induced condensation of gas-phase species, then the average of the 240 lowest RIC spectra (1/6 of the sampled particles) would be the most likely spectrum to show the presence of *m/z* 252. Since it does not (see Figure 1a), significant sampling induced condensation is absent.

Another possible problem is that fluctuations in the intensity of the laser interaction due to laser power fluctuations, off-center hits, and hot spots in the laser beam could cause variations in the RIC of the individual spectra and may cause the evolution that we observe in the mass spectra. In ref 12, we presented micrographs of particles sampled from the flame that showed both extremes of particles, transparent droplets, and black mature soot aggregates. We observed the same types of particles under the microscope in the LMMS study we performed from the same experiment. These particle extremes were observed optically without a laser; therefore the laser is not affecting the evolutionary extremes. Moreover, as yet unpublished LMMS measurements on the clear droplets with 250 times more laser intensity than used in our real-time experiments only show PAH and PAH

(18) Korre, S. C.; Klien, M. T.; Quann, R. J. *Ind. Eng. Chem. Res.* **1991**, *30*, 2021.

fragment ions; they do not show carbon cluster ions. We conclude that the laser is not inducing carbonization and therefore is not responsible for the evolution as a function of RIC.

Resonance ejection was used to extend the mass range of the ion trap mass spectrometer by a factor of 2.883 employing a supplementary 124.9 kHz AC voltage to the end-cap electrodes¹⁹ to study fullerene formation. One thousand soot particles were analyzed for fullerene formation in the extended mass range (m/z 300–865) under identical flame conditions. The average of the individual particle spectra is shown in Figure 2a. A continuation of the PAH progression above m/z 300 is revealed. Under our experimental conditions, the observed pyrolytic addition process did not continue in such a manner to produce very large PAH molecules (i.e., PAH containing on the order of 60 or more carbon atoms) presumably because the smaller hydrocarbon reaction partners within the soot particles are consumed.

Little evidence of fullerene formation is observed here. This result was not surprising since McKinnon, Bell, and Barkley⁶ found no evidence of extractable fullerenes (C_{60} and C_{70}) from soot produced under essentially our same conditions from an acetylene torch with no oxygen flow; therefore, we did not expect to see appreciable fullerene production. However, if the high-mass region of this spectrum is examined under $\times 20$ magnification (see the inset in Figure 2a), there is a distribution of ions with a signal-to-noise ratio of about 3 that suggests fullerenes are being formed in small trace level quantities. We see them because laser ionization mass spectrometry is one of the most sensitive techniques for observing fullerenes. However, because McKinnon, Bell, and Barkley⁶ found no detectable fullerenes in their extracted soot from an acetylene torch, we decided not to attempt to quantify the fullerene formation in the soot by extraction methods by similar available methods.

From our observations of the soot carbonization process under identical flame conditions made on the same day,¹² we know that two-thirds of the soot particles measured here are PAH-containing and one-third are mature or carbonaceous soot. Approximately half of the PAH-containing particle spectra show significant intensity above m/z 300 due to pyrolysis-induced growth of the PAHs in the particle phase. Since the majority of fullerene observations were from pyrolysis of carbon, it was expected that the fullerenes would be found in the mature soot fraction. To test this hypothesis, the particle spectra were sorted into two bins. The spectra with the majority of spectral intensity in the low-mass region between m/z 300 and 400 were collected into one bin. The 369 spectra in this bin were averaged and the results are shown in Figure 2b. The same PAH progression that dominates the average in Figure 2a is seen here with approximately one-third the spectra. This result agrees with our observation of the soot carbonization process in Figure 1. Examination of the baseline in the high-mass region of Figure 2b under higher magnification ($\times 20$) reveals no evidence of fullerene formation confirming the supposition that the fullerenes are found in the mature soot fraction.

The remaining 631 spectra were placed in the other bin. The bin was further culled to remove spectra with low RICs. Finally, these spectra were again culled leaving only spectra that showed evidence of fullerene formation in the form of high-mass lines with a repeating peak separation of approximately 24 mass units. The 196 spectra left in the bin were averaged and the results are shown in Figure 2c. (For the sake of completeness, the

average of the 435 rejected spectra was examined for a coherent ion formation pattern, but none was found.) Our measured fullerene ion distribution from the particle phase is similar to that found directly in the gas phase of a benzene flame at reduced pressure.²⁰ The m/z values of the spectral features in the benzene flame experiments did not shift when benzene- d_6 was burned indicating that the gas-phase-produced fullerenes do not contain hydrogen. However, our results indicate the production of hydrogenated low-mass fullerenes (C_{32} – C_{56}) from the particle phase as evidenced by the intensity in the m/z values immediately greater than the fullerene peaks. These so-called hydrogenated low-mass fullerenes seen here probably have incompletely closed cage structures. The similarity of this hydrogenation pattern to the carbon cluster ion pattern in Figure 1e,f is evidence that the species observed in Figure 2c–e are carbon clusters and not PAHs. If they were PAHs then the ion distributions would be Gaussian about the PAH masses due to rapid pyrolysis-induced hydrogen exchange as seen in Figure 1b–d.

The particle spectra whose average is seen in Figure 2c were further culled for spectra with significant C_{60} intensity in an attempt to observe fullerene evolution. Of the 196 fullerene-containing particle spectra, 31 were found to have significant C_{60} ion intensity. The average of the 31 C_{60} -containing particle spectra is presented in Figure 2d and the average of the remaining 165 fullerene spectra is presented in Figure 2e. From the above observations, the point where the mature soot begins to form is the branching point where fullerene formation becomes viable. During the hydrogen exchange/carbon skeleton rearrangement process, two “PAH” molecules can react with each other to form a larger more energetically stable unit. (The word PAH is in quotes to denote the uncertainty of the structure.) These more stable fullerene units are observed in Figure 2e. The intensity distribution of the fullerenes in Figure 2e appears to correlate with the intensity distributions of the PAHs in Figure 1d if one assumes the fullerenes are formed by fusing pairs of PAHs with concurrent hydrogen loss.

The pronounced lack of mass spectral intensity from the PAHs observed in Figures 2d and 2e and the lack of fullerene structure in Figure 2b (see inset) suggest the formation of the fullerenes in Figure 2e must occur after the pyrolytic addition process to form the higher mass PAH and as the carbonization process changed the PAHs to carbonaceous soot. There was no evidence for the formation of significant amounts of PAHs with the same number of carbon atoms as are in the fullerenes (e.g., $C_{60}H_n$ PAH) seen in Figure 2. There was also no evidence for significant formation of fullerenes through the buildup of bowl-like structures by the addition of acetylene or other small hydrocarbons in the manner suggested by Pope et al.²¹ Buildup of bowl-like structures is not the likely the production method of the fullerenes observed in our experiments, in part for the lack of evidence of any intermediate from the process such as corannulene (m/z 250) in the averaged mass spectra, but primarily because the fullerene synthesis observed here is taking place in the particle phase where the PAH distribution is relatively constant, suggesting that there is not much free small hydrocarbon material with which to build up these bowl structures. It was concluded that the initial formation of the low-mass fullerenes, under our flame conditions, happened as a result of the carbonization process of the PAHs permitting binary combination and restructuring of the joined “PAHs”.

(20) Gerhardt, Ph.; Lyffler, S.; Homann, K. H. *Chem. Phys. Lett.* **1987**, 137, 306.

(21) Pope, C. J.; Marr, J. A.; Howard, J. B. *J. Phys. Chem.* **1993**, 97, 11001.

(19) *Practical Aspects of Ion Trap Mass Spectrometry*; March, R. E., Todd, J. F. J., Eds.; CRC Press: Boca Raton, FL, 1995; Vol. II, pp 3–47.

The soot carbonization process was found by Dobbins et al.²² to occur between 1500 and 2000 K. Consequently, fullerene formation in the particle phase probably also occurs in this temperature range. The optimal temperatures for forming fullerenes from graphite were found to be much higher, 3000 K or higher.²³ The optimal temperature for the formation of C₆₀ ions in the gas phase of an acetylene/oxygen flame was observed to be approximately 2150 K.² Taylor and co-workers²⁴ have observed that vapor phase pyrolysis of naphthalene under argon produced C₆₀ and C₇₀ at approximately 1300 K. Howard²⁵ observed in flames that produce both fullerenes and soot that fullerene production significantly lags soot formation. Our results that fullerenes are formed in the particle phase while the carbonization process is occurring, in combination with the above observations, support the suggestion of Baum et al.² that gas-phase fullerenes may be created by a second mechanism in the particle phase at a temperature lower than 2150 K and subsequently liberated from the particle surface. This would allow their observation of apparent gas-phase formation at the previously reported optimum higher temperature.

The fullerenes in Figure 2d show evidence of hydrogenation (or incomplete cage closure) that appeared to be mass dependent. The smaller fullerenes show the highest degree of hydrogenation with up to 18–21 hydrogen atoms attached. (Remember each line in the mass spectrum has a integrated width of 2.88 mass units.) The degree of hydrogenation decreases with increasing mass. Presumably this occurs because the number of dangling bonds decreases with increasing mass as suggested by Smalley²⁶ in explanation of the observed “forbidden zone” and because there is a large amount of labile hydrogen in the soot particle that can react with these dangling bonds. This observation also makes one wonder why there was no corresponding increase in intensity of the C₋₃₂H_n ions caused by the stabilizing influence of the labile hydrogen attaching to the dangling bonds. Perhaps there is a more fundamental reason for the existence of Smalley’s “forbidden zone”.²⁶ More work is needed to resolve this observation.

Comparison of the local intensity distributions of the hydrogenated fullerenes in Figure 2d,e yields insight into the formation mechanism of the higher mass fullerenes such as C₆₀ and C₇₀. There was a pronounced increase in the C₄₄, C₅₀, C₆₀, and C₇₀ ion intensities in Figure 2d compared to Figure 2e. The observation of strong intensity for these ions in Figure 2d is in accordance with the results in the graphite vaporization experiments.¹ It therefore seems reasonable to assume that the soot particles that make up the averaged spectra in Figure 2d were more “mature” than those that make up the average in Figure 2e. Furthermore, it seems reasonable to assume that the particle composition in Figure 2e was the precursor to the average in Figure 2d. Observation of the change in the local ion distributions of the low-mass hydrogenated fullerenes suggested that C₆₀ and C₇₀ were more readily formed from the dehydrogenated low-mass fullerenes. Moreover, it was apparent that hydrogenated C₆₀ and C₇₀ ions (or incompletely closed C₆₀ and C₇₀) were not very abundant. It was therefore apparent that rearrangement following the reaction of the low-mass fullerenes to form C₆₀ and C₇₀ was very rapid. Consequently, it was not clear whether the reaction partner of the low-mass fullerene in the

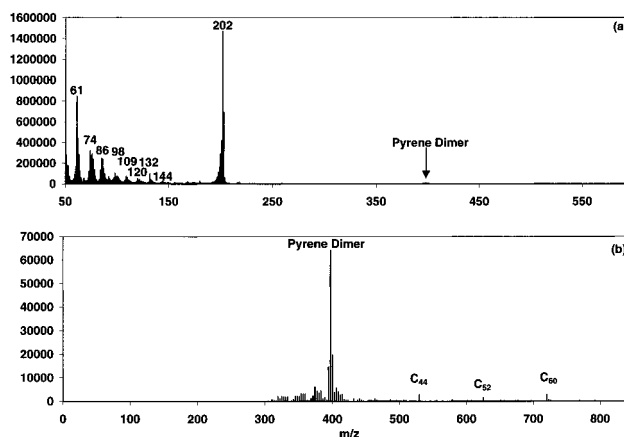


Figure 3. The averaged mass spectra from laser-induced pyrolysis of individual pure pyrene particles: (a) low mass spectrum and (b) high mass spectrum from the same sample. All masses below m/z 300 were expelled from the trap to enhance the sensitivity to the higher masses.

formation of C₆₀ and C₇₀ is another low-mass fullerene, other “PAHs”, or a graphitic carbon fragment. More work is required to answer this question. However, the above results suggest the possibility of controlled fullerene synthesis in an analogous condensed-phase medium.

It is now time to address the issue of whether the evolution processes that we observed here are the result of condensation from the gas phase on to the soot particle due to the sampling process, the laser ablation process, or formation by flame-induced pyrolysis of the soot particle. It was demonstrated in ref 12 that our sampling technique thoroughly mixes the particles and gases sampled from the entire cross section of the flame on the submillisecond time scale (i.e., shortly after entering the sampling tube). Adulteration of the particle by aggregation and/or condensation due to the sampling process cannot be significant because this type of adulteration would destroy the evolutionary pattern seen in Figure 1; these processes should occur uniformly regardless of particle composition. For the same reason, significant deposition of fullerenes on to the soot particles from the gas phase would destroy the evolutionary pattern observed here and fullerenes would then be seen on every particle. This observation is true for deposition during sampling as well as deposition in the flame during the evolution of the soot. Substantial fullerene formation where the fullerene ion intensities are on the same scale as the PAH ion intensities (compare Figures 1d and 2d) during laser ablation of the particle is also unlikely due to the short (<1 μs) interaction time during the ablation process. This does not mean that fullerene formation cannot happen on the time scale of the duration of the laser plume if the laser heats the particle enough. To test this, we examined the effects of laser-induced pyrolysis on pure pyrene particles. Panels a and b in Figure 3 show the spectral averages in the low and high mass range, respectively, from laser-induced pyrolysis of individual pure pyrene particles taken with the same laser at $\sim 1 \times 10^8$ W/cm². Figure 3a reveals that hydrogen exchange between the pyrene molecules, fragmentation, and a small amount of dimerization can be laser induced. No substantial dimerization was observed from the acetylene soot particles. Figure 3b shows that fullerene production from pure pyrene particles can also be induced by laser pyrolysis. The highest C₆₀ ion intensity in the individual particle mass spectra that make the average in Figure 3b is 15 000 units. This is more than 3 orders of magnitude less intense than the pyrene ion intensity in Figure 3a. The fullerene ion intensities and the PAH ion intensities observed from the acetylene soot particle were

(22) Dobbins, R. A.; Govatzidakis, G. J.; Lu, W.; Schwartzman, A. F.; Fletcher, R. A. *Combust. Sci. Technol.* **1996**, *121*, 103.

(23) Singh, H.; Srivastava, M. *Energy Sources* **1995**, *17*, 615.

(24) Taylor, R.; Langley, G. J.; Kroto, H. W.; Walton, D. R. M. *Nature* **1993**, *366*, 728.

(25) Howard, J. B. *Twenty-Fourth Symposium (International) on Combustion*; The Combustion Institute: Pittsburgh, 1992; p 933.

(26) Smalley, R. E. *Acc. Chem. Res.* **1992**, *25*, 101.

of the same order of magnitude (see Figures 1d and 2d). Given the difference in the dimerization and fullerene intensities between our laser pyrolysis and flame results, we do not believe that the observed fullerenes from the acetylene soot are coming from laser-induced pyrolysis of the PAHs in the soot particles. Soot particles were also sampled from the flame through the same sampling tube at the same height using an impactor. The collected particles were examined with an optical microscope and revealed both semitransparent globules and black soot aggregates. This confirms that the carbonization process happens without the laser. For the sake of completeness, we decided to look for fullerene production from graphite particles. No fullerene production was observed from graphite particles under the same laser conditions used in the pure pyrene particle experiments. Consequently, we concluded that the fullerenes observed in our particle mass spectra were not created from the laser. Thus by process of elimination, we believe the formation mechanism for the particle phase fullerenes must then be flame-induced pyrolysis of the PAH-containing particles.

It can be correctly argued that pure pyrene and graphite particles are not necessarily good analogues for soot particles produced in the flames. We concede that laser-induced fullerene production from the acetylene soot particle is within the realm of possibility; but significant production is not very probable given the lack of dimer ions in our results. Moreover, the observed mechanism of PAH dimerization to form low-mass fullerenes and hydrogenated or partially open low-mass fullerenes followed by further reaction with another large species is more conducive to condensed phase formation than it is to gas-phase formation.

The above results are not consistent with the mechanisms suggested in the literature for fullerene formation in the gas phase of the flame. Fullerene formation in the condensed phase for relatively large particles (~ 750 nm) is unlikely to occur by sequential addition of acetylene followed by loss of hydrogen as suggested by Pope and co-workers²¹ and by Frenklach and Ebert.²⁷ Our results show that large amounts of acetylene or any other small hydrocarbon are not condensed in the PAH-containing particle because there is little pyrolysis-induced growth of the PAHs (see Figure 1) and there is a lack of significant amounts of the more stable intermediates ($C_{20}H_{10}$, $C_{30}H_{10}$, $C_{40}H_{10}$, $C_{50}H_{10}$, and $C_{60}H_{10}$) compared to the "PAHs". In the same publication,²¹ Pope and co-workers also suggested a coagulation mechanism for the formation of C_{60} from $C_{30}H_9$ yielding $C_{60}H_{18}$ followed by dehydrogenation. Our results also cannot support this mechanism due to the lack of evidence of significant quantities of $C_{60}H_{18}$ or any similar large mass (i.e., 60 carbon) PAH and due to the observed change in the hydrogenated low-mass fullerene distribution between panels d and e in Figures 2.

Fullerenes have been previously found to form in the gas phase with and without the presence of soot; therefore, PAHs were determined to be their precursors.^{2,3} However, when soot was present the full spectrum of fullerenes was formed while in its absence C_{50} , C_{60} , and C_{70} were formed preferentially.³ Hydrogenated (or opened caged) fullerenes were not observed in the gas phase and it was therefore suggested that they could be found in young soot particles that could act as reactors for

fullerenes.² Our results support this suggestion. However, this group also suggests that fullerenes were formed through a "concerted zipper mechanism" and that the smaller fullerenes cannot be formed without oxidative degradation. Our results in Figure 2d,e demonstrate formation of the smaller fullerenes without oxidative degradation. Furthermore, our results show that dimerization of the PAHs to form the low-mass fullerenes occurs as a result of rapid hydrogen exchange leading to carbon skeleton rearrangement with concurrent hydrogen loss. This process is not described by the "concerted zipper mechanism".

Conclusions

The results of our investigation have reveal substantial evidence for the formation of fullerenes in the condensed or particle phase for the first time. We observed fullerene formation in the particle phase to be the result of the carbonization process of the PAH-containing particles. Because the carbonization process occurs between 1500 and 2000 K, we suggest that fullerenes might be created in the particle phase and subsequently liberated into the gas phase by increasing temperature. The carbonization process is characterized by the onset of rapid hydrogen exchange among the PAH and other hydrogen-containing species. As the rate of hydrogen exchange builds up, there is also evidence of pyrolytic addition to the PAH from smaller hydrocarbon species slightly shifting the distribution toward higher mass. Under our experimental conditions, the pyrolytic addition process did not continue, presumably because the smaller hydrocarbon reaction partners within the particles were consumed. The rate of hydrogen exchange continued to build until there was a sudden loss of the PAH population in the particle and a corresponding growth of the carbon cluster ion intensities. The hydrogen loss/gain became so severe that carbon-carbon bond rearrangement became facile enough for the PAHs to be converted into other species. We suggest this to be the branching point between fullerene and carbonaceous soot formation.

Fullerene formation was determined to be preceded by binary combination of the "PAH" to form low-mass fullerenes. The structure of the reacting "PAHs" was not clear, but it is most probably rapidly changing in terms of carbon-carbon skeletal structure and degree of hydrogenation. This soup of rapid rearrangement allows the low-mass fullerenes to form because they are minimal energy structures. The low-mass fullerenes were determined to be the precursors to C_{60} and C_{70} ; however, their reaction partners in this process are uncertain. They may be more dehydrogenated PAH, carbon-containing fragments from the pyrolysis process, or other low-mass fullerenes. They are not low-mass hydrocarbons. More work is needed to understand this step in the mechanism.

Acknowledgment. The authors would like to thank Dr. Alexandru C. Lazar for performing the pyrene measurements. This research was sponsored by the Office of Research and Development, U.S. Department of Energy, under contract DE-AC05-96OR22464 with Oak Ridge National Laboratory managed by Lockheed Martin Energy Research Corp.

(27) Frenklach, M.; Ebert, L. B. *J. Phys. Chem.* **1988**, *92*, 561.